SPANDIDOS PUBLICATIONS INTERNATIONAL JOURNAL OF MOLECULAR MEDICINE 31: 1087-1096, 2013

Transplantation of Flk-1$^+$ human bone marrow-derived mesenchymal stem cells promotes behavioral recovery and anti-inflammatory and angiogenesis effects in an intracerebral hemorrhage rat model

XIN-JIE BAO[1*], FU-YI LIU[1,2*], SHAN LU[4*], QIN HAN[3], MING FENG[1], JUN-JI WEI[1], GUI-LIN LI[1], ROBERT CHUN-HUA ZHAO[3] and REN-ZHI WANG[1]

[1]Department of Neurosurgery, Peking Union Medical College Hospital, Chinese Academy of Medical Sciences and Peking Union Medical College, Beijing 100730; [2]Department of Neurosurgery, Second Affiliated Hospital of the Medical School of Zhejiang University, Hangzhou 310009; [3]Institute of Basic Medical Sciences and School of Basic Medicine, Center of Excellence in Tissue Engineering, Chinese Academy of Medical Sciences and Peking Union Medical College, Beijing 100005; [4]China National Center for Biotechnology Development, Beijing 100036, P.R. China

Received November 10, 2012; Accepted January 30, 2013

DOI: 10.3892/ijmm.2013.1290

Abstract. Mesenchymal stem cells (MSCs) have been successfully used for the treatment of experimental intracerebral hemorrhage (ICH). However, the neuroprotective mechanisms through which MSCs improve neurological functional recovery are not fully understood. In the present study, we tested the hypothesis that treatment with MSCs inhibits inflammation after ICH and reduces subsequent brain injury. Adult rats subjected to stereotaxic injection of collagenase VII were transplanted with a subpopulation of human bone marrow-derived MSCs (hBMSCs), termed fetal liver kinase (Flk)-1$^+$ hBMSCs, or saline into the ipsilateral brain parenchyma 1 day after ICH. Significant recovery of behavior was noted in the Flk-1$^+$ hBMSC-treated rats beginning 3 days after ICH compared with the control group. Brain water content was significantly decreased in the ipsilateral hemispheres of the Flk-1$^+$ hBMSC-treated rats when compared with the controls 3 days after ICH. The relative hemorrhage volume was reduced 55 days after Flk-1$^+$ hBMSC treatment. However, this change was not statistically significant. Flk-1$^+$ hBMSCs significantly inhibited the proliferation of rat peripheral blood mononuclear cells (rPBMCs) induced in a mixed lymphocyte reaction. Consistently, we found a significant anti-inflammatory effect of Flk-1$^+$ hBMSCs on the ICH brain, including a decrease in neutrophil infiltration and microglial activation in the peri-ICH area, and downregulation of inflammatory mediators, such as interleukin (IL)-1β, IL-2, IL-4, IL-6, and tumor necrosis factor (TNF)-α. In addition, Flk-1$^+$ hBMSC treatment significantly increased vascular density in the peri-ICH area, and transplanted Flk-1$^+$ hBMSCs were found to be incorporated into the cerebral vasculature 55 days after transplantation. Overall, these data suggest an essential role for Flk-1$^+$ hBMSCs in reducing inflammatory infiltration, promoting angiogenesis, and improving functional recovery after ICH in rats.

Introduction

Intracerebral hemorrhage (ICH) represents at least 10% of all cases of stroke, with a 30-day mortality ranging from 35 to 52% (1,2). Nearly 30% of patients with ischemic stroke have secondary ICH (3), particularly as a major complication of thrombolytic therapy (4). Currently, medical therapy for patients with ICH is generally limited to supportive care or neurosurgical evacuation of the hematoma. Therefore, development of alternative therapies for ICH is important.

ICH induces brain injury due to local tissue deformation and subsequent pathological changes such as inflammation, excitotoxicity and apoptosis (5). Hematoma-induced injury mainly involves mechanical disruption of neurons and glia, followed by mechanical deformation causing oligemia, neurotransmitter release, mitochondrial dysfunction and membrane depolarization. A secondary cascade of injury is started by products of coagulation and hemoglobin breakdown, in particular thrombin, which leads to microglia activation and neutrophil infiltration 4 h after ICH (6). Increasing evidence suggest that ICH-induced inflammation is a key factor in secondary brain damage. The inflammatory cascade comprises both cellular and molecular components. Blood components, including erythrocytes, neutrophils, macrophages, thrombin, and plasmin immediately infiltrate the brain after ICH. The inflammatory responses

Correspondence to: Dr Ren-Zhi Wang, Department of Neurosurgery, Peking Union Medical College Hospital, Chinese Academy of Medical Sciences and Peking Union Medical College, 1 Shuai-Fu-Yuan Hutong, Dong-Cheng, Beijing 100730, P.R. China
E-mail: wangrz@126.com

*Contributed equally

Key words: angiogenesis, bone marrow, inflammation, intracerebral hemorrhage, mesenchymal stem cells

involve enzyme activation, mediator release, inflammatory cell migration and glial activation (7). Activated microglia and infiltrating neutrophils release products that induce breakdown of the blood-brain barrier, vasogenic oedema, and apoptosis in neurons and glia (6). Therefore, anti-inflammatory approaches may improve the outcome of ICH, and anti-inflammatory pharmacologic therapies have been investigated to reduce the brain injury after ICH (5,8,9).

Mesenchymal stem cells (MSCs), a heterogeneous population of plastic-adherent cells, have been successfully used for the treatment of experimental ICH (10-12). In our previous study, we showed that transplantation of human bone marrow-derived MSCs (hBMSCs) increased glucose metabolic activity in the cortex and basal ganglia in the hemorrhagic boundary zone using serial ^{18}F-FDG PET scans, leading to neurological recovery in *Macaca fascicularis* monkey models (12). However, the clinical application of stem cell therapy in stroke has been delayed since the neuroprotective mechanisms by which MSCs improve functional recovery remain largely unknown. Recently, MSCs are receiving more and more attention based on the observation that they can exert immunoregulatory activity both *in vitro* and *in vivo* (13-15). MSCs have been reported to have therapeutic effects by downregulating inflammation in a variety of diseases such as graft-versus-host disease after kidney transplant (16), lung injury (17), myocardial infarction (18) and experimental autoimmune encephalomyelitis (19). Therefore, MSC treatment may inhibit inflammation after ICH and reduce subsequent brain injury. To examine this hypothesis, we used a subpopulation of hBMSCs, termed fetal liver kinase (Flk)-1$^+$ hBMSCs, which share most features of MSCs and possess marked differentiation potential, even after being expanded for >50 cell doublings (20,21). Flk-1$^+$ hBMSCs may represent a very early population in the hierarchy of stem cell development. This is the first stem cell product approved by the State Food and Drug Administration (SFDA) of China, and the feasibility and safety of Flk-1$^+$ hBMSC transplantation were evaluated in rhesus monkeys and humans (22). Understanding the mechanisms underlying the beneficial effects of BMSC therapy may greatly enhance its translation to the clinic.

Materials and methods

Cell culture, flow cytometry and karyotype analysis. Bone marrow was obtained from the iliac aspirates of healthy male volunteers after informed consent was obtained. Human BMSCs were used in accordance with the procedures approved by the Human Experimentation and Ethics Committee. As described (37), ~20 ml of bone marrow was obtained from each volunteer and diluted with the same volume of normal saline. Mononuclear cells were separated using lymphocyte separation medium and density gradient centrifugation (1.077 g/cm^3). The cells were plated at the density of 3x10^5/cm^2 in Dulbecco's modified Eagle's medium/nutrient mixture F-12 (Invitrogen, Carlsbad, CA, USA) supplemented with 40% MCDB-201 medium (Sigma, St. Louis, MO, USA), 10% fetal bovine serum (FBS; Hyclone, Logan, UT, USA), 10 ng/ml epidermal growth factor, 10 ng/ml platelet-derived growth factor, 100 U/ml phytomycin and 100 U/ml penicillin (all were from Sigma), and cultured at 37˚C in a humidified atmosphere containing 5% CO_2. After 24 h, non-adherent cells were washed and removed. The medium was replaced with the same fresh medium every third day. The cells were digested with pancreatic enzyme (Invitrogen) and passaged upon reaching 80% confluence.

At the fifth passage, hBMSCs were collected, counted, and analyzed by flow cytometry for phycoerythrin anti-human phycoerythrin-CD29, -CD105, -CD31, -Flk-1, -CD34, -CD44 and human leukocyte antigen-DR (HLA-DR) expression (Becton-Dickinson Biosciences, San Diego, CA, USA).

For karyotype analysis, metaphases were prepared from methanol/acetic acid (3:1) fixed cells. Slides were hybridized by spectral karyotyping. At least 20 metaphase cells were analyzed from each hBMSC preparation. Breakpoints were assigned based on G-banded karyotype.

Mixed lymphocyte reaction. Rat peripheral blood mononuclear cells (rPBMCs) from individual Sprague-Dawley rats were pooled and used as responder cells. Human peripheral blood mononuclear cells (hPBMCs; 3x10^5/well) from a healthy volunteer and Flk-1$^+$ hBMSCs (5x10^4/well) were used as stimulator cells in 96-well round-bottom plates. Responder rPBMCs (3x10^5/well) were added to irradiated (15 Gy) stimulator hPBMCs or Flk-1$^+$ hBMSCs in RPMI-1640 medium containing 10% FBS (supplied by Peking Union Medical College). In the mitogen proliferative assay, responder rPBMCs (3x10^5/well) were incubated with 3 μg/ml concanavalin A (ConA; Sigma). Furthermore, rPBMCs (3x10^5/well) containing ConA were added to Flk-1$^+$ hBMSCs in 96-well plates. Following 5 days of incubation at 37˚C in a humidified atmosphere containing 5% CO_2, cells were pulsed with ^{3}H-thymidine (1 μCi/well; supplied by China Atomic Energy Research Institute) for the last 18 h, harvested, and counted with a Microβ 1450 Trilux liquid scintillation counter (Wallac Inc., Gaithersburg, MD, USA). Results were expressed in counts per minute (cpm) and presented as the means obtained from triplicate cultures.

ICH model and groups. All animal procedures were performed in accordance with guidelines issued by the Committee on Animal Research of Peking Union Medical College Hospital and were approved by the Institutional Ethics Committee (Peking Union Medical College, Beijing). Adult male Sprague-Dawley rats weighing 190-210 g were used. ICH was induced via the stereotaxic intrastriatal injection of collagenase type VII (Sigma), as described previously (9). In brief, rats were anesthetized with 10% chloral hydrate (400 mg/kg, i.p.; Sigma). Rectal temperature was maintained at 37˚C throughout the surgical procedure using a heating lamp. Animals were placed in a stereotaxic frame and an incision was made exposing the bregma. One burr hole was drilled at the injection site: anterior-posterior (AP) -0.2 mm, mediolateral (ML) 2.9 mm, and dorsoventral (DV) 6.0 mm from the dura. Collagenase type VII (0.4 IU) in 2 μl saline was injected at a rate of 0.7 μl/min. The needle was left in place for 2 min prior to withdrawal. The rats recovered from anesthesia and were returned to their cages with free access to food and water. On 1 day after ICH, the modified neurological severity score (mNSS) test was calculated based on a series of motor, sensory, balance and reflex tests (33). Rats subjected to ICH with mNSS 10-14 were selected and were

randomly assigned to two groups: i) the Flk-1$^+$ hBMSC-treated group (ICH + hBMSCs, n=65) and ii) the saline control group (ICH + saline, n=67).

Cell transplantation. On day 1 after ICH, rats were anesthetized as described above and received transplantation of Flk-1$^+$ hBMSCs or saline. Animals were placed in a stereotaxic frame and burr holes were drilled at three injection sites: site 1, AP 1.6 mm, ML 2.5 mm and DV 4.0 mm from dura; site 2, AP 0.2 mm, ML 2.9 mm and DV 4.0 mm from dura; site 3, AP -1.8 mm, ML 3.8 mm and DV 4.5 mm from dura. Approximately 2x10^5 Flk-1$^+$ hBMSCs in 15 μl saline or an equal volume of saline was injected at a rate of 1 μl/min. Following injections, the needle was left in place for 2 min prior to withdrawal.

Behavioral testing. The mNSS test was performed at 1, 3, 7, 14, 28, 42 and 56 days after ICH by an investigator blinded to the experimental groups (n=12 for each group). The mNSS test is a composite of motor, sensory, balance and reflex tests. Neurological function is graded on a scale of 0-18 (normal score, 0; maximal deficit score, 18). A single point is awarded for a specific abnormal behavior or for the lack of a tested reflex; thus, the higher the score the more severe the injury (33).

Brain water content. The brain water content was measured 3 days after ICH (n=6 for each group), as previously described (9). In brief, the rats were over-anesthetized. The brains were removed immediately, and divided into the ipsilateral and contralateral hemispheres. Each brain sample was placed on a piece of aluminum foil, and immediately weighed on an electronic analytical balance to obtain the wet weight, then dried at 110˚C for 24 h to obtain the dry weight. The brain water content was calculated using the following equation: % Water = (wet weight - dry weight)/wet weight x 100.

Tissue processing. On days 3, 7, 14, 28 and 56 following ICH, rats (n=6 for each group, respectively) were intracardially perfused with chilled saline followed by 4% paraformaldehyde in 0.01 M PBS (pH 7.4). The brains were collected and postfixed in 4% paraformaldehyde at 4˚C overnight, then transferred to 30% sucrose in PBS at 4˚C for cryoprotection. Coronal sections (8 μm) were taken from a +2.0 to -2.0 mm area around the bregma using a vibratome (Leica, Wetzlar, Germany), thaw-mounted on gelatine-coated slides and stored at -80˚C until processing.

Nissl staining and peroxidase immunohistochemistry. Nissl staining was used to detect neurons according to standard methods (38). In brief, the sections were incubated in 1% cresyl violet for 30 sec, decolorized in acetic acid, and then dehydrated and covered. Diaminobenzidine peroxidase immunohistochemistry was used to label myeloperoxidase (MPO)$^+$ cells (neutrophils). Briefly, slices were blocked with normal goat serum for 30 min at 37˚C, and then incubated in rabbit anti-MPO IgG (1:200; Abcam, Cambridge, UK) at 4˚C overnight. After three washes in PBS, sections were incubated in horseradish peroxidase (HRP)-conjugated goat anti-rabbit IgG (1:200; ZSJQ Corp., Beijing, China) for 30 min at 37˚C, and developed using a DAB kit.

Immunofluorescence histochemistry. Slices were blocked with normal goat serum for 30 min at 37˚C, and then incubated in mouse anti-ED1 IgG (a marker for macrophage and activated microglia, 1:150; Millipore, Temecula, CA, USA) or mouse anti-NeuN IgG (a marker for neurons, 1:200; Millipore) at 4˚C overnight. After three washes in PBS, sections were incubated in the dark for 30 min at 37˚C with Rhodamine-conjugated or FITC-conjugated goat anti-mouse IgG (1:150). After washing, sections were covered with mounting medium containing 4',6'-diamino-2-phenylindole (DAPI) (both were from ZSJQ Corp.).

Double-label immunofluorescence was used to analyze the survival and differentiation of Flk-1$^+$ hBMSCs. MAB1281 (mouse anti-human nuclear monoclonal antibody, Millipore) is a marker for human cells (39). In the present study, it was used to detect Flk-1$^+$ hBMSCs. To visualize the cellular colocalization of MAB1281 and cell type-specific markers in the same cells, each section was incubated at 4˚C overnight in the primary MAB1281 (1:100) with microtubule-associated protein 2 (MAP-2) (a neuron marker; rabbit monoclonal IgG, 1:200; Millipore), glial fibrillary acidic protein (GFAP) (an astrocyte marker; rabbit monoclonal IgG, 1:400; Abcam), or von Willebrand factor (vWF) (an endothelial marker; rabbit monoclonal IgG, 1:200; Abcam). After washing, sections were incubated in the dark for 30 min at 37˚C in FITC-conjugated goat anti-mouse IgG (1:150) with Rhodamine-conjugated goat anti-rabbit IgG (1:150) (both were from ZSJQ Corp.).

Terminal deoxynucleotidyltransferase (TdT)-mediated dUTP-biotin nick-end labeling (TUNEL) staining. TUNEL staining was performed using the *In Situ* Cell Death Detection kit (TMR red; Roche Diagnostics, Mannheim, Germany) according to the manufacturer's instructions. In brief, slices were first incubated in permeabilization solution containing 0.1% sodium citrate and 0.1% Triton X-100 at 4˚C for 2 min. Sections were then incubated with TdT enzyme in reaction buffer containing TMR red labeled dUTP at 37˚C for 60 min. The negative control was incubated in reaction buffer without the TdT enzyme. After washing with wash buffer, sections were covered with mounting medium containing DAPI (ZSJQ Corp.).

Hematoxylin and eosin staining. On day 56 following ICH, rats were deeply anesthetized with chloral hydrate and were fixed by transcardial perfusion with saline, followed by 4% paraformaldehyde. The brains were collected and embedded in paraffin. The brain tissue was dissected into 6 pieces of 2-mm coronal blocks with rodent brain matrix. A series of adjacent 6-μm sections were cut from each block (33). The brain sections were stained with hematoxylin and eosin and photographed with a microscope (Zeiss, Oberkochen, Germany). Relative hemorrhage volume was analyzed with ImagePro Plus software (Media Cybernetics, Inc., Bethesda, MD, USA). The indirect lesion area, in which the intact area of the ipsilateral hemisphere was subtracted from the area of the contralateral hemisphere, was calculated. Relative hemorrhage volume was presented as the percentage of the volume of the indirect lesion compared with the contralateral hemisphere (40).

Quantitative real-time RT-PCR. Total RNA was extracted from ipsilateral brain tissues (Fig. 5A) by TRIzol reagent

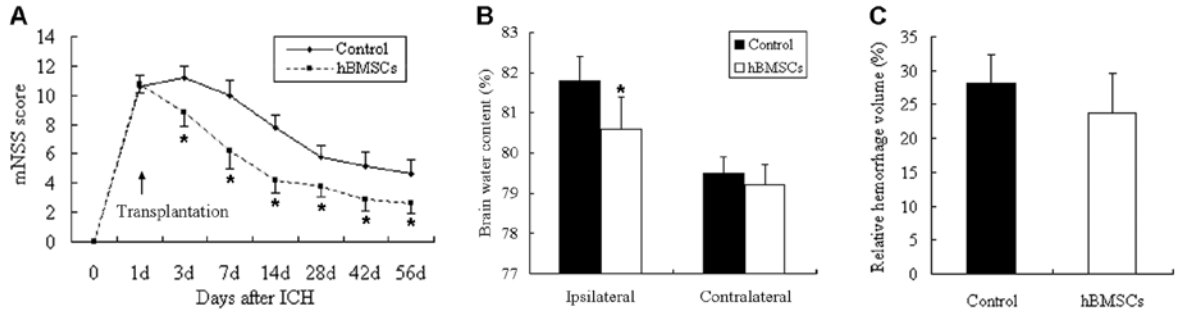

Figure 1. Transplantation of Flk-1$^+$ human bone marrow-derived mesenchymal stem cells (hBMSCs) promoted functional recovery, decreased brain water content, and reduced hemorrhage volume in rats after intracerebral hemorrhage (ICH). (A) The mNSS test results from 1 to 56 days after ICH. Significant differences were detected at each time-point starting 3 days after ICH (2 days after transplantation) in the Flk-1$^+$ hBMSC-treated group. (B) Brain water content was significantly decreased in the ipsilateral hemispheres of the Flk-1$^+$ hBMSC-treated rats when compared with the values in the controls 3 days after ICH. (C) The relative hemorrhage volume was reduced 55 days after Flk-1$^+$ hBMSC treatment. However, this change was not statistically significant. Data are expressed as means ± SD; *P<0.05, n=6.

(Invitrogen). RNA concentrations were determined by absorbance readings at 260 nm with GeneQuant (Amersham Biosciences, Amersham, UK), and 1 μg total RNA was reverse transcribed to cDNA using the RevertAid™ First Strand cDNA Synthesis kit with oligo(dT) primers (Fermentas, Hanover, MD, USA). PCR amplification was performed in a 50-μl volume containing 2 μl of each primer and 25 μl SYBR-Green qPCR mix (Toyobo, Osaka, Japan). The amplification procedure consisted of 50˚C for 2 min, 95˚C for 10 min and 40 cycles of amplification reactions at 95˚C for 15 sec, and at 60˚C for 1 min. The primers used were as follows: interleukin (IL)-1β (100 bp) forward, 5'-CAGCTTTCGACAGTGAGGAGAA-3' and reverse, 5'-CTCATCTGGACAGCCCAAGTC-3'; IL-2 (100 bp) forward, 5'-GCCACAGAATTGAAACATCTTCAG-3' and reverse, 5'-GCGTCTTCCAAGTGAAAGCTTT-3'; IL-4 (100 bp) forward, 5'-ACCTCCGTGCTTGAAGAACAA-3' and reverse, 5'-CATTCACGGTGCAGCTTCTC-3'; IL-6 (100 bp) forward, 5'-CAGCGATGATGCACTGTCAGA-3' and reverse, 5'-TCAATAGGCAAATTTCCTGGTTATATC-3'; tumor necrosis factor (TNF)-α (100 bp) forward, 5'-TGTACCTTATCTACTCCCAGGTTCTCT-3' and reverse, 5'-CTCCTGGTATGAAATGGCAAATC-3'; R-actin β (93 bp) forward, 5'-CAACCGTGAAAAGATGACCCA-3' and reverse, 5'-AATGCCAGTGGTACGACCAGA-3'. R-actin β cDNA was used as a control. Relative expression between a given sample and a reference sample was calculated using the $2^{-\Delta\Delta Ct}$ method.

Quantification. The sections were examined under a fluorescence microscope (Eclipse 80i; Nikon, Tokyo, Japan) or under a confocal laser scanning microscope (Leica TCS SP2; Leica, Wetzlar, Germany). Images were collected and analyzed with ImagePro Plus software (Media Cybernetics, Inc., Bethesda, MD, USA) based on evaluation of an average of 3 slides (8-μm thick, 72-μm interval, every 10th slide) for each animal. We counted the total number of MAB1281-positive cells in the consistently selected area, and the percentage of MAB1281-positive cells colocalized with cell type-specific markers (MAP-2, GFAP and vWF) by double staining was investigated in terms of where the transplanted cells were located. The number of MPO$^+$ and ED1$^+$ cells around the hemorrhagic lesion, and NeuN$^+$, Nissl$^+$ and TUNEL$^+$ cells in the ipsilateral cortical area were counted for six random high-power fields in each section, and these data were averaged.

Statistical analysis. Data are presented as means ± SD and analyzed by SPSS 10.0 software (SPSS, Inc., Chicago, IL, USA). For the behavioral test, analysis of variance (ANOVA) was used to test the group effect by the repeated time of assessments. The results of the mixed lymphocyte reaction were analyzed by ANOVA. Brain water content, relative hemorrhage volume, immunohistochemistry, and quantitative real-time RT-PCR data were analyzed by the Student's 2-tailed unpaired t-test. A P-value of <0.05 was considered to indicate a statistically significant result.

Results

The mNSS test was assessed before rats were selected and randomly grouped. In this way, we tried to control the quality and minimize variations of the models. One hundred and twenty of the 132 ICH rats survived. Among the 12 animals that died prematurely, 5 were in the Flk-1$^+$ hBMSC-treated group and 7 were in the control group.

Characteristics and karyotype analysis of hBMSCs. The phenotypes of hBMSCs used in this study were positive for Flk-1, CD29, CD44, CD105 and CD106 and were negative for HLA-DR, CD31 and CD34. They displayed the capacity for multi-lineage differentiation into adipocytes, osteoblasts and chondrocytes (23). Flk-1$^+$ hBMSCs at the fifth passage were used for karyotype analysis, which was conducted to validate chromosome stability. No trisomy, tetraploidy or chromosome rearrangement was observed (24).

Neurological behavior, brain water content, and hemorrhage volume. The mNSS test was compared between the Flk-1$^+$ hBMSC-treated and control rats. There was no difference in neurological outcome before cell transplantation; however, significant functional improvement appeared in the Flk-1$^+$ hBMSC-treated group at each time point starting at 3 days after ICH compared with the control group (P<0.05) (Fig. 1A).

Brain water content in the ipsilateral (hemorrhagic) hemisphere at 3 days post-ICH was significantly reduced in the

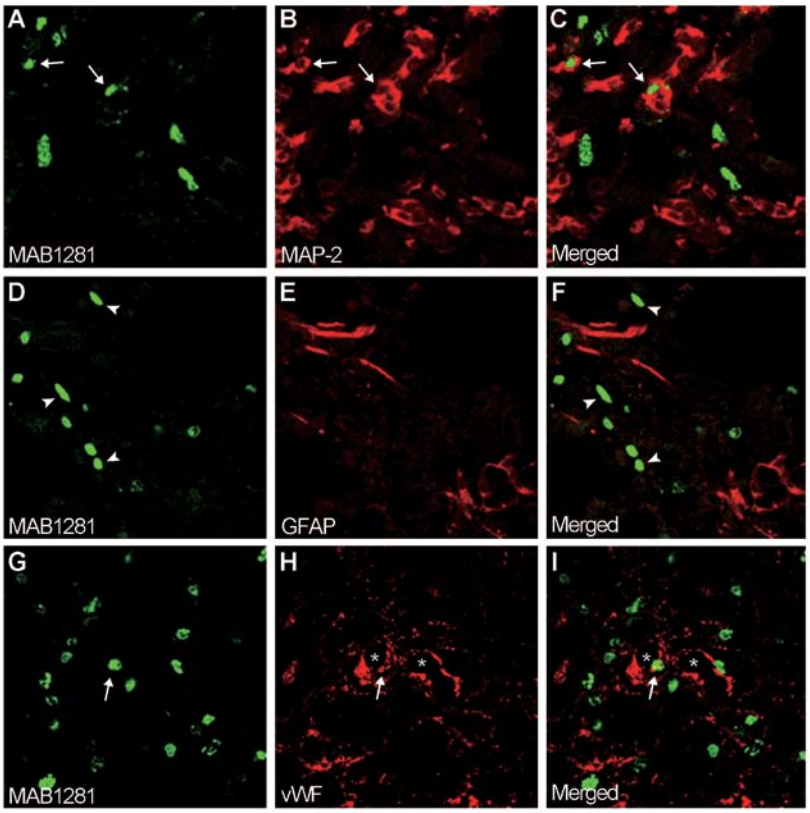

Figure 2. (A-I) Double-label immunohistochemical responses of Flk-1$^+$ human bone marrow-derived mesenchymal stem cells (hBMSCs) in the recipient rat brain are shown. Immunofluorescence (green) indicates that (A and G) MAB1281-reactive hBMSCs express phenotypes of (B and C) the neuron marker microtubule-associated protein-2 (MAP-2) and (H and I) vascular endothelial marker, von Willebrand factor (vWF) (arrows). However, (D) no MAB1281-reactive hBMSCs were detected to express (E and F) astrocyte marker, glial fibrillary acidic protein (GFAP) (arrowheads). (A-I) Original magnification, x40. Asterisks represented blood vessels.

Flk-1$^+$ hBMSC-treated group (80.6±0.8%) compared with the controls (81.8±0.6%) (P<0.05) (Fig. 1B). However, no difference was observed in the contralateral hemisphere (79.5±0.4% in the control group and 79.2±0.5% in the Flk-1$^+$ hBMSC-treated group) (P>0.05) (Fig. 1B).

Following hematoxylin and eosin staining, hemorrhagic lesions mainly appeared in the striatum 56 days after ICH. Hemorrhagic core tissues were transformed into cysts. The damaged tissue consisted of a central cavity surrounded by a scar border. Although lower hemorrhagic volume was detected in the Flk-1$^+$ hBMSC-treated rats (23.8±5.8%) when compared with that in the controls (28.2±4.2%), no significant difference was found between the two groups (P>0.05) (Fig. 1C).

Identification of donor cells in recipients. Flk-1$^+$ hBMSCs survived and the majority of the cells were distributed close to the hemorrhagic boundary zone 55 days after transplantation. Few Flk-1$^+$ hBMSCs were observed in the contralateral hemisphere. Double-label immunohistochemistry revealed that Flk-1$^+$ hBMSCs (Fig. 2A and G) were reactive for neuron marker, MAP-2 (Fig. 2B and C), and endothelial marker, vWF (Fig. 2H and I); however, no Flk-1$^+$ hBMSCs (Fig. 2D) were colocalized with astrocyte marker, GFAP (Fig. 2E and F). The hemorrhagic boundary zone was divided into three different areas (striatum, cortex and corpus callosum). In the striatum, the percentages of Flk-1$^+$ hBMSCs that expressed MAP-2, vWF and GFAP were ~4.3, 1.2 and 0% respectively. In the cortex,

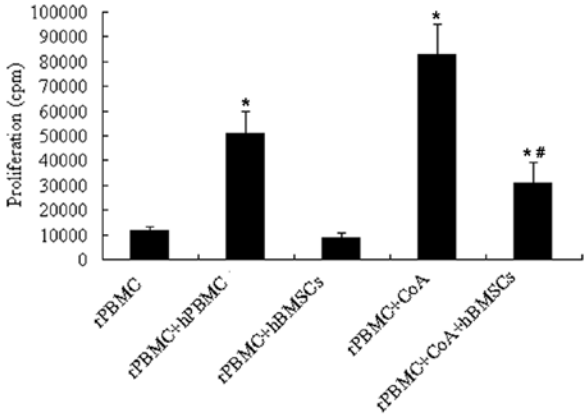

Figure 3. Flk-1$^+$ human bone marrow-derived mesenchymal stem cells (hBMSCs) exerted immunomodulation function *in vitro*. Human peripheral blood mononuclear cells (hPBMCs) and concanavalin A (CoA) induced proliferation of rat peripheral blood mononuclear cells (rPBMC); however, Flk-1$^+$ hBMSCs inhibited the response when cocultured with rPBMCs or rPBMCs/CoA. Data are expressed as means ± SD. Significant difference from rPBMCs, *P<0.05; significant difference from rPBMCs/CoA, $^\#$P<0.05.

the percentages of Flk-1$^+$ hBMSCs that expressed MAP-2, vWF and GFAP were ~5.8, 2.5 and 0%, respectively. In the corpus callosum, the percentages of Flk-1$^+$ hBMSCs that expressed MAP-2, vWF and GFAP were ~1.6, 1.6 and 0%, respectively. The control rats were evaluated, and no hBMSCs were detected.

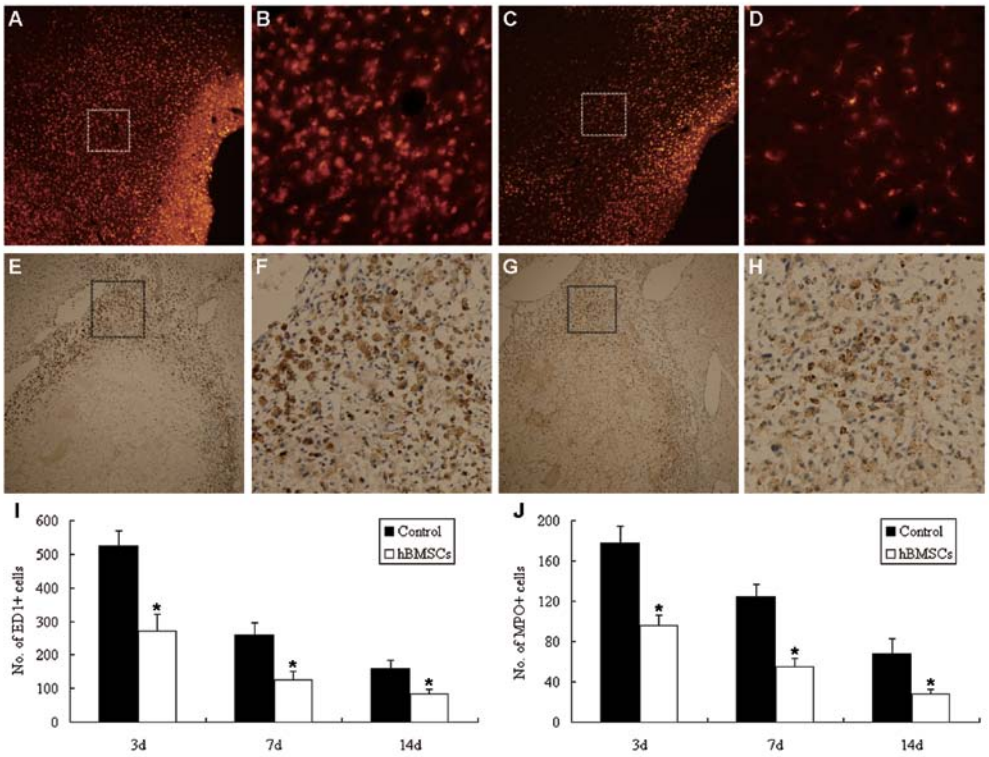

Figure 4. Anti-inflammatory effects of Flk-1$^+$ human bone marrow-derived mesenchymal stem cell (hBMSC) treatment in rats after intracerebral hemorrhage (ICH). Immunofluorescence staining of ED1 in (A) the control group and (C) the Flk-1$^+$ hBMSC-treated group. (B and D) Amplified images of the boxed areas in A and C. Peroxidase immunohistochemistry of myeloperoxidase (MPO) in (E) the control group and (G) the Flk-1$^+$ hBMSC-treated group. (F and H) Amplified images of the boxed areas in E and G. Quantification of (I) ED1$^+$ and (J) MPO$^+$ cells in the hemorrhagic boundary zone. Original magnification: A, C, E and G, x10; B, D, F and H, x40. Data are expressed as means ± SD; *P<0.05, n=6 at each time point.

Immunomodulatory effect of Flk-1$^+$ hBMSCs in vitro. To confirm the *in vitro* immunomodulatory effect of Flk-1$^+$ hBMSCs, Flk-1$^+$ hBMSCs and hPBMCs were added to mixed lymphocyte cultures of rPBMCs, respectively. Human PBMCs induced the proliferation of rPBMCs, whereas Flk-1$^+$ hBMSCs did not elicit a proliferative response of rPBMCs. Furthermore, Flk-1$^+$ hBMSCs significantly inhibited the proliferation of rPBMCs induced by ConA (P<0.05) (Fig. 3).

Anti-inflammatory effect of Flk-1$^+$ hBMSCs in vivo. Microglial activation and neutrophil infiltration are main inflammatory responses after ICH, with a peak at 3 to 7 days (25). In the present study, microglia and neutrophils were shown by ED1 and MPO staining, respectively. ED1$^+$ and MPO$^+$ cells in the hemorrhagic boundary zone were significantly decreased in the Flk-1$^+$ hBMSC-treated rats when compared with the controls (P<0.05) (Fig. 4A-J).

Real-time reverse transcription-polymerase chain reaction assay (RT-PCR) was used to analyze changes in the levels of inflammatory mediators, including IL-1β, IL-2, IL-4, IL-6 and TNF-α. On day 3, the mRNA levels of IL-1β, IL-2, IL-4, IL-6 and TNF-α were all downregulated in the Flk-1$^+$ hBMSC-treated rats. On days 7 and 14, significantly lower levels of IL-2 and TNF-α were detected in the rats transplanted with Flk-1$^+$ hBMSCs (Fig. 5B-F).

Flk-1$^+$ hBMSC treatment promotes angiogenesis and reduces cell apoptosis. To determine whether Flk-1$^+$ hBMSC treatment induces angiogenesis in the hemorrhagic boundary zone, we performed immunofluorescence staining and blood vessel density assays. Quantitative analysis of blood vessel density examined by vWF immunofluorescence showed that ICH rats treated with Flk-1$^+$ hBMSCs had significantly increased neovasculature in the hemorrhagic boundary region when compared with the controls (P<0.05) (Fig. 6A-C).

TUNEL staining was used to investigate neuron apoptosis. The number of TUNEL$^+$ cells in the cortical hemorrhagic boundary was significantly decreased in the Flk-1$^+$ hBMSCs-treated rats compared with this value in the controls (P<0.05) (Fig. 7A-C). The number of survival neurons in the cortical hemorrhagic boundary, stained by NeuN (Fig. 7D and E) or Nissl (Fig. 7G and H), was higher in rats receiving Flk-1$^+$ hBMSCs when compared with this value in controls at 56 days after ICH (P<0.05) (Fig. 7F and I).

Discussion

In the present study, we demonstrated that transplantation of Flk-1$^+$ hBMSCs into ipsilateral brain parenchyma reduced inflammatory infiltration and promoted angiogenesis in a rat ICH model, which was accompanied by the reduction in brain edema, a decrease in cell apoptosis and improved neurological function.

Similar to MSCs, Flk-1$^+$ hBMSCs have unique immunologic characteristics, such as low immunogenicity and immunoregulatory property. They express negligible levels

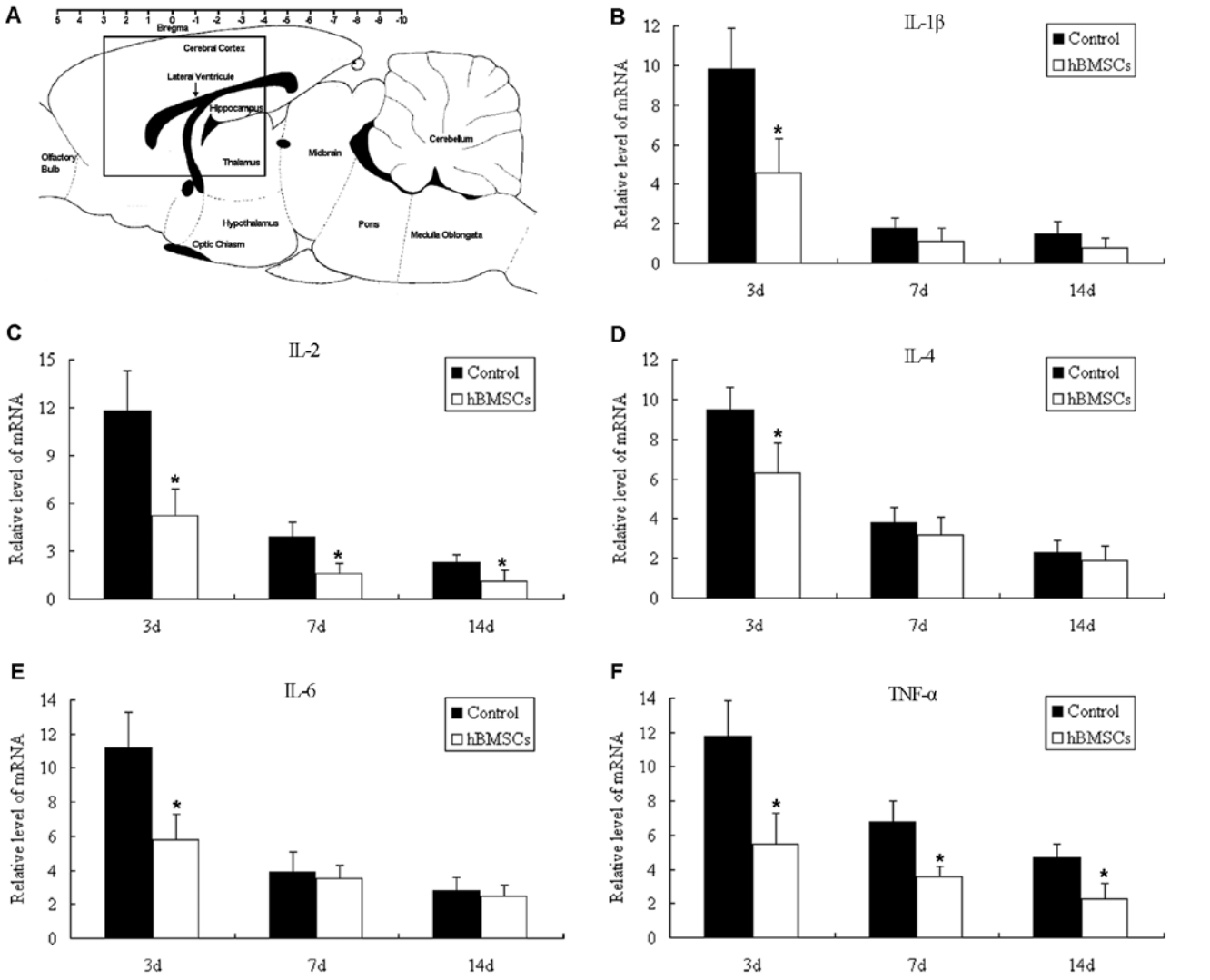

Figure 5. Real-time RT-PCR analysis of interleukin (IL)-1β, IL-2, IL-4, IL-6, and tumor necrosis factor (TNF)-α mRNA levels in the hemorrhagic rat brain. (A) The sagittal section shows the area (box) where brain tissue was selected for RT-PCR. The expression of (B) IL-1β, (D) IL-4 and (E) IL-6 was downregulated 3 days after intracerebral hemorrhage (ICH) in rats receiving Flk-1$^+$ human bone marrow-derived mesenchymal stem cells (hBMSCs). Lower levels of both (C) IL-2 and (F) TNF-α were expressed at 3, 7 and 14 days in the Flk-1$^+$ hBMSC-treated rats when compared with the levels in the controls. Data are expressed as means ± SD; *P<0.05, n=6 at each time point.

of major histocompatibility complex (MHC) class I and no MHC class II or Fas ligand, nor do they express CD80, CD86, CD40 or CD40L (13-15). It has been demonstrated that MSCs produce hepatocyte growth factor and transforming growth factor-β (TGF-β) to mediate T-cell suppression, while other studies have emphasized that cell contact is also important in the immunoregulatory property of MSCs (26). In our previous study, we found that Flk-1$^+$ BMSCs, partly via cell-cell contact, drive mature dendritic cells to differentiate into a novel Jagged-2-dependent regulatory dendritic cell population and escape their apoptotic fate, and thus revealed a new mechanism of their immunoregulation (15). In the present study, Flk-1$^+$ hBMSCs significantly inhibited the proliferation of rPBMCs induced in a mixed lymphocyte reaction. Consistently, we found a significant anti-inflammatory effect of Flk-1$^+$ hBMSCs in the ICH brain, including decreased neutrophil infiltration and microglial activation in the perihematomal areas, and downregulation of inflammatory mediators, IL-1β, IL-2, IL-4, IL-6 and TNF-α. These immunological characteristics may allow for their use in allogeneic or xenogeneic transplantation without any immunosuppressant and they may have an anti-inflammatory effect on brain damage after ICH or other immunological diseases (16,19,23). These findings suggest that Flk-1$^+$ hBMSCs are likely to interact with inflammatory cascades after ICH. However, further research is required to identify the intrinsic anti-inflammatory mechanisms of Flk-1$^+$ hBMSCs *in vivo*.

Our previous studies revealed that Flk-1$^+$ hBMSCs differentiate into brain parenchymal cells both *in vitro* (20,21) and *in vivo* (27,28), and replacement of neural cells was often considered to be the main goal of cell therapy for stroke (29). However, the number of BMSCs that survived after transplantation was relatively small and was miniscule compared to the ~25-30% hemispheric brain tissue damage observed after ICH. Furthermore, only a small percentage of BMSCs express neural protein, too few to replace the injured tissue (10,11), while expression of phenotypic brain cell markers does not indicate true differentiation and may be a misinterpretation

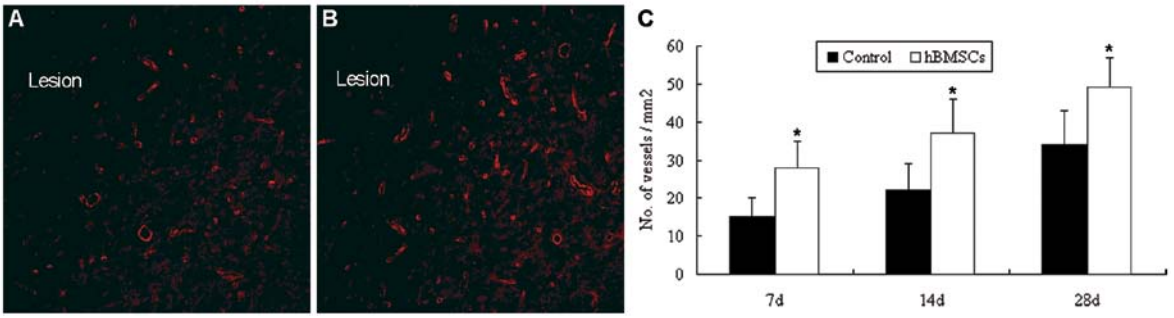

Figure 6. Flk-1$^+$ human bone marrow-derived mesenchymal stem cell (hBMSC) treatment induces angiogenesis in the hemorrhagic boundary zone. Immunofluorescence staining of von Willebrand factor (vWF) in (A) the control group and (B) the Flk-1$^+$ hBMSC-treated group 7, 14 and 28 days following ICH. (C) Quantification of cerebral blood vessel density in the hemorrhagic boundary zone. (A and B) Original magnification, x20. Data are expressed as means ± SD; *P<0.05, n=6 at each time point.

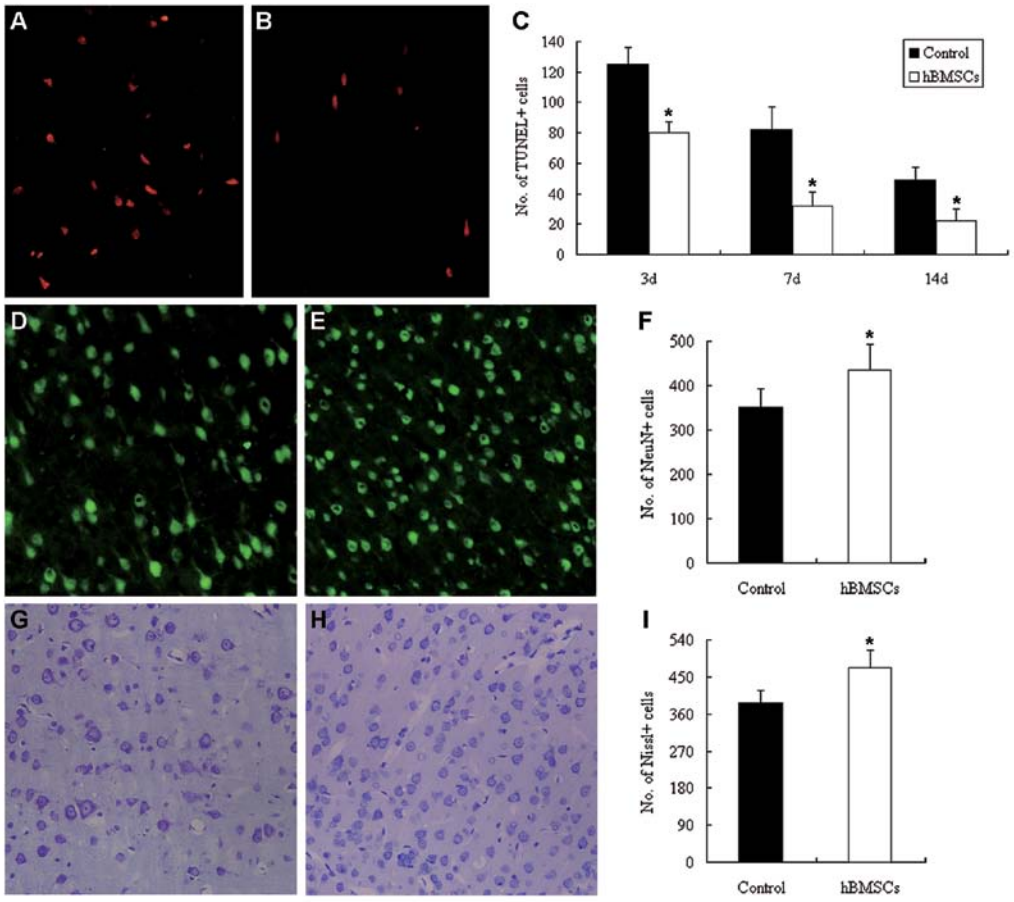

Figure 7. Transplantation of Flk-1$^+$ human bone marrow-derived mesenchymal stem cells (hBMSCs) reduces the apoptosis of neurons in the cortical hemorrhagic boundary. The number of TUNEL$^+$ cells was strongly reduced in rats transplanted with (B) Flk-1$^+$ hBMSCs when compared with (A) the controls. (C) Quantification of TUNEL$^+$ cells in the cortical hemorrhagic boundary. The number of neurons was significantly decreased in the control group when compared with this value in the Flk-1$^+$ hBMSC-treated group. Immunofluorescence staining of NeuN and Nissl staining in the (D and G) control group and (E and H) Flk-1$^+$ hBMSCs-treated group. Quantification of (F) NeuN$^+$ and (I) Nissl$^+$ cells in the cortical hemorrhagic boundary. Original magnification; A, B, D, E, G and H, x20. Data are expressed as means ± SD; *P<0.05, n=6 at each time point.

of spontaneous cell fusion (30,31). In the present study, the number of Flk-1$^+$ hBMSCs that survived 55 days after transplantation was relatively small and only a small percentage of Flk-1$^+$ hBMSCs expressed proteins phenotypic of neural-like cells. The death of Flk-1$^+$ hBMSCs was primarily attributed to the deleterious microenvironment after ICH. Functional recovery was observed within days after Flk-1$^+$ hBMSC treatment. It is highly unlikely that these cells integrated into the cerebral tissue and made appropriate connections within days after transplantation.

Another mechanism that mediated the benefit of Flk-1$^+$ hBMSCs following ICH may be attributed to

angiogenesis. We previously reported that Flk-1$^+$ hBMSCs transdifferentiate into vascular endothelial cells both *in vitro* and *in vivo* (20,21). Additionally, transplantation of Flk-1$^+$ hBMSCs to the rat ischemic brain significantly promoted vascular endothelial cell proliferation and induced angiogenesis in the ischemic boundary zone (24,28). In the present study, we observed that Flk-1$^+$ hBMSCs were located in the vessel wall and differentiated into vascular endothelial cells in the hemorrhagic boundary region, indicating that increased angiogenesis following Flk-1$^+$ hBMSC treatment may be associated with direct incorporation into cerebral vasculature. However, the percentage of Flk-1$^+$ hBMSCs that expressed an endothelial phenotype was extremely small, consistent with previous studies (32,33). These findings indicate that Flk-1$^+$ hBMSC-induced angiogenesis may largely depend on the proliferation of endogenous endothelial cells or recruitment of endothelial progenitor cells toward the hemorrhagic brain, rather than the transdifferentiation of grafted Flk-1$^+$ hBMSCs. BMSC-induced proliferation of endothelial cells is, at least partially, attributed to trophic factors (32). Flk-1$^+$ BMSCs secrete multiple trophic factors in rat brain, including vascular endothelial growth factor (VEGF), brain-derived neurotrophic factor (BDNF), neurotrophin-3 (NT-3), insulin-like growth factor-1 (IGF-1), basic fibroblast growth factor (bFGF), glia-derived neurotrophic factor (GDNF) and TGF (24,28). VEGF is the most important mitogen in the process of angiogenesis (34), and VEGF expression was significantly upregulated in the brain of rats receiving Flk-1$^+$ hBMSCs in our previous studies (24,28). Furthermore, BMSC treatment of cerebral ischemia was found to promote vascular stabilization and to decrease VEGF-induced blood-brain barrier leakage, by increasing angiopoietin-1/Tie2 and VEGF/Flk-1 expression (35).

In conclusion, BMSCs show promise as a potential therapy for restoration of function after cerebral hemorrhage. However, most stem cell-based therapies remain in the early stages of development. Recommendations and guidelines for translation of laboratory studies with stem cells to patients have been published following the 'Stem Cell Therapies as an Emerging Paradigm in Stroke (STEPS)' conference (36). Understanding the mechanisms underlying the beneficial effects of these therapies will greatly enhance their translation to the clinic.

Acknowledgements

This study was supported by a grant from the National High Technology Research Project (2011AA020112 and 2006AA02A115) and the National Natural Science Foundation of China (81200916 and 81100869).

References

1. Heiskanen O: Treatment of spontaneous intracerebral and intracerebellar hemorrhages. Stroke 24: I94-I95, 1993.
2. Qureshi AI, Tuhrim S, Broderick JP, Batjer HH, Hondo H and Hanley DF: Spontaneous intracerebral hemorrhage. N Engl J Med 344: 1450-1460, 2001.
3. Lyden PD and Zivin JA: Hemorrhagic transformation after cerebral ischemia: mechanisms and incidence. Cerebrovasc Brain Metab Rev 5: 1-16, 1993.
4. Hacke W, Kaste M, Bluhmki E, *et al*: Thrombolysis with alteplase 3 to 4.5 hours after acute ischemic stroke. N Engl J Med 359: 1317-1329, 2008.
5. Aronowski J and Hall CE: New horizons for primary intracerebral hemorrhage treatment: experience from preclinical studies. Neurol Res 27: 268-279, 2005.
6. Qureshi AI, Mendelow AD and Hanley DF: Intracerebral haemorrhage. Lancet 373: 1632-1644, 2009.
7. Wang J and Doré S: Inflammation after intracerebral hemorrhage. J Cereb Blood Flow Metab 27: 894-908, 2007.
8. Kim J, Lee S, Kon C, *et al*: Systemic transplantation of human adipose stem cells attenuated cerebral inflammation and degeneration in a hemorrhagic stroke model. Brain Res 1183: 43-50, 2007.
9. Lee S, Chu K, Jung K, *et al*: Anti-inflammatory mechanism of intravascular neural stem cell transplantation in haemorrhagic stroke. Brain 131: 616-629, 2008.
10. Seyfried D, Ding J, Han Y, Li Y, Chen J and Chopp M: Effects of intravenous administration of human bone marrow stromal cells after intracerebral hemorrhage in rats. J Neurosurg 104: 313-318, 2006.
11. Zhang H, Huang Z, Xu Y and Zhang S: Differentiation and neurological benefit of the mesenchymal stem cells transplanted into the rat brain following intracerebral hemorrhage. Neurol Res 28: 104-112, 2006.
12. Feng M, Zhu H, Zhu Z, *et al*: Serial ^{18}F-FDG PET demonstrates benefit of human mesenchymal stem cells in treatment of intracerebral hematoma: a translational study in a primate model. J Nucl Med 52: 90-97, 2011.
13. Deng W, Han Q, Liao L, *et al*: Allogeneic bone marrow-derived Flk-1$^+$Sca-1$^-$ mesenchymal stem cells leads to stable mixed chimerism and donor-specific tolerance. Exp Hematol 32: 861-867, 2004.
14. Xu G, Zhang L, Ren G, Yuan Z, Zhang Y, Zhao RC and Shi Y: Immunosuppressive properties of cloned bone marrow mesenchymal stem cells. Cell Res 17: 240-248, 2007.
15. Zhang B, Liu R, Shi D, *et al*: Mesenchymal stem cells induce mature dendritic cells into a novel Jagged-2-dependent regulatory dendritic cell population. Blood 113: 46-57, 2009.
16. Tan J, Wu W, Xu X, *et al*: Induction therapy with autologous mesenchymal stem cells in living-related kidney transplants: a randomized controlled trial. JAMA 307: 1169-1177, 2012.
17. Saito S, Nakayama T, Hashimoto N, *et al*: Mesenchymal stem cells stably transduced with a dominant-negative inhibitor of CCL_2 greatly attenuate bleomycin-induced lung damage. Am J Pathol 179: 1088-1094, 2011.
18. Williams AR and Hare JM: Mesenchymal stem cells: biology, pathophysiology, translational findings, and therapeutic implications for cardiac disease. Circ Res 109: 923-940, 2011.
19. Morando S, Vigo T, Esposito M, *et al*: The therapeutic effect of mesenchymal stem cell transplantation in experimental autoimmune encephalomyelitis is mediated by peripheral and central mechanisms. Stem Cell Res Ther 3: 3, 2012.
20. Fang B, Liao L, Shi M, Yang S and Zhao RC: Multipotency of Flk1$^+$CD34$^-$ progenitors derived from human fetal bone marrow. J Lab Clin Med 143: 230-240, 2004.
21. Fang B, Shi M, Liao L, Yang S, Liu Y and Zhao RC: Multiorgan engraftment and multilineage differentiation by human fetal bone marrow Flk1$^+$/CD31$^-$/CD34$^-$ progenitors. J Hematother Stem Cell Res 12: 603-613, 2003.
22. Liu L, Sun Z, Chen B, *et al*: Ex vivo expansion and in vivo infusion of bone marrow-derived Flk-1$^+$CD31$^-$CD34$^-$ mesenchymal stem cells: feasibility and safety from monkey to human. Stem Cells Dev 15: 349-357, 2006.
23. Zhou H, Guo M, Bian CJ, *et al*: Efficacy of bone marrow-derived mesenchymal stem cells in the treatment of sclerodermatous chronic graft-versus-host disease: clinical report. Biol Blood Marrow Transplant 16: 403-412, 2010.
24. Bao X, Feng M, Wei J, *et al*: Transplantation of Flk-1$^+$ human bone marrow-derived mesenchymal stem cells promotes angiogenesis and neurogenesis after cerebral ischemia in rats. Eur J Neurosci 34: 87-98, 2011.
25. Gong C, Hoff JT and Keep RF: Acute inflammatory reaction following experimental intracerebral hemorrhage in rat. Brain Res 871: 57-65, 2000.
26. Nauta AJ and Fibbe WE: Immunomodulatory properties of mesenchymal stromal cells. Blood 110: 3499-3506, 2007.
27. Li J, Zhu H, Liu Y, *et al*: Human mesenchymal stem cell transplantation protects against cerebral ischemic injury and upregulates interleukin-10 expression in *Macaca fascicularis*. Brain Res 1334: 65-72, 2010.
28. Bao X, Wei J, Feng M, *et al*: Transplantation of human bone marrow-derived mesenchymal stem cells promotes behavioral recovery and endogenous neurogenesis after cerebral ischemia in rats. Brain Res 1367: 103-113, 2011.

29. Li Y, Chen J, Chen XG, *et al*: Human marrow stromal cell therapy for stroke in rat: neurotrophins and functional recovery. Neurology 59: 514-523, 2002.
30. Terada N, Hamazaki T, Oka M, *et al*: Bone marrow cells adopt the phenotype of other cells by spontaneous cell fusion. Nature 416: 542-545, 2002.
31. Castro RF, Jackson KA, Goodell MA, Robertson CS, Liu H and Shine HD: Failure of bone marrow cells to transdifferentiate into neural cells in vivo. Science 297: 1299, 2002.
32. Chen J, Zhang ZG, Li Y, *et al*: Intravenous administration of human bone marrow stromal cells induces angiogenesis in the ischemic boundary zone after stroke in rats. Circ Res 92: 692-699, 2003.
33. Shen LH, Li Y, Chen J, *et al*: One-year follow-up after bone marrow stromal cell treatment in middle-aged female rats with stroke. Stroke 38: 2150-2156, 2007.
34. Schott RJ and Morrow LA: Growth factors and angiogenesis. Cardiovasc Res 27: 1155-1161, 1993.
35. Zacharek A, Chen J, Cui X, *et al*: Angiopoietin1/Tie2 and VEGF/Flk1 induced by MSC treatment amplifies angiogenesis and vascular stabilization after stroke. J Cereb Blood Flow Metab 27: 1684-1691, 2007.
36. Stem Cell Therapies as an Emerging Paradigm in Stroke Participants: The STEPS Participants: Stem cell therapies as an emerging paradigm in stroke (STEPS): bridging basic and clinical science for cellular and neurogenic factor therapy in treating stroke. Stroke 40: 510-515, 2009.
37. Han Q, Sun Z, Liu L, Chen B, Cao Y, Li K and Zhao RC: Impairment in immuno-modulatory function of $Flk1^{+}$ $CD31^{-}$ $CD34^{-}$ MSCs from MDA-RA patients. Leuk Res 31: 1469-1478, 2007.
38. Parent JM, Valentin VV and Lowenstein DH: Prolonged seizures increase proliferating neuroblasts in the adult rat subventricular zone-olfactory bulb pathway. J Neurosci 22: 3174-3188, 2002.
39. Henriksson HB, Svanvik T, Jonsson M, Hagman M, Horn M, Lindahl A and Brisby H: Transplantation of human mesenchymal stems cells into intervertebral discs in a xenogeneic porcine model. Spine 34: 141-148, 2009.
40. Swanson RA, Morton MT, Tsao-Wu G, Savalos RA, Davidson C and Sharp FR: A semiautomated method for measuring brain infarct volume. J Cereb Blood Flow Metab 10: 290-293, 1990.